ARTICLE

Association of *APOE4* and Clinical Variability in Alzheimer Disease With the Pattern of Tau- and Amyloid-PET

Renaud La Joie, PhD, Adrienne V. Visani, BS, Orit H. Lesman-Segev, MD, Suzanne L. Baker, PhD, Lauren Edwards, BS, Leonardo Iaccarino, PhD, David N. Soleimani-Meigooni, MD, Taylor Mellinger, BS, Mustafa Janabi, PhD, Zachary A. Miller, MD, David C. Perry, MD, Julie Pham, BA, Amelia Strom, BS, Maria Luisa Gorno-Tempini, MD, PhD, Howard J. Rosen, MD, Bruce L. Miller, MD, William J. Jagust, MD, and Gil D. Rabinovici, MD

Correspondence
Dr. La Joie
Renaud.lajoie@ucsf.edu

Neurology® 2021;96:e650-e661. doi:10.1212/WNL.0000000000011270

Abstract

Objective

To assess whether Alzheimer disease (AD) clinical presentation and *APOE4* relate to the burden and topography of β-amyloid (Aβ) and tau pathologies using in vivo PET imaging.

Methods

We studied 119 Aβ-positive symptomatic patients aged 48–95 years, including 29 patients with logopenic variant primary progressive aphasia (lvPPA) and 21 with posterior cortical atrophy (PCA). Pittsburgh compound B (PiB)–Aβ and flortaucipir (tau)–PET standardized uptake value ratio (SUVR) images were created. General linear models assessed relationships between demographic/clinical variables (phenotype, age), *APOE4*, and PET (including global cortical and voxelwise SUVR values) while controlling for disease severity using the Clinical Dementia Rating Sum of Boxes.

Results

PiB-PET binding showed a widespread cortical distribution with subtle differences across phenotypes and was unrelated to demographic/clinical variables or *APOE4*. Flortaucipir-PET was commonly elevated in temporoparietal regions, but showed marked phenotype-associated differences, with higher binding observed in occipito-parietal areas for PCA, in left temporal and inferior frontal for lvPPA, and in medial temporal areas for other AD. Cortical flortaucipir-PET binding was higher in younger patients across phenotypes ($r = -0.63$, 95% confidence interval [CI] −0.72, −0.50), especially in parietal and dorsal prefrontal cortices. The presence of *APOE4* was associated with a focal medial temporal flortaucipir-SUVR increase, controlling for all other variables (entorhinal: + 0.310 SUVR, 95% CI 0.091, 0.530).

Conclusions

Clinical phenotypes are associated with differential patterns of tau but not amyloid pathology. Older age and *APOE4* are not only risk factors for AD but also seem to affect disease expression by promoting a more medial temporal lobe–predominant pattern of tau pathology.

RELATED ARTICLE

Editorial
Spatial Distribution of Tau and β-Amyloid Pathologies and Their Role in Different Alzheimer Disease Phenotypes
Page 191

From the Memory and Aging Center, Department of Neurology, Weill Institute for Neurosciences (R.L.J., A.V.V., O.H.L.-V., L.E., L.I., D.N.S.-M., T.M., Z.A.M., D.C.P., J.P., A.S., M.L.G.-T., H.J.R., B.L.M., G.D.R.), and Department of Radiology and Biomedical Imaging (G.D.R.), University of California, San Francisco; Department of Diagnostic Imaging (O.H.L.-V.), Sheba Medical Center, Tel Hashomer, Ramat Gan, Israel; Molecular Biophysics and Integrated Bioimaging Division (S.L.B., M.J., W.J.J., G.D.R.), Lawrence Berkeley National Laboratory; and Helen Wills Neuroscience Institute (W.J.J., G.D.R.), University of California Berkeley.

Go to Neurology.org/N for full disclosures. Funding information and disclosures deemed relevant by the authors, if any, are provided at the end of the article.

Glossary

Aβ = β-amyloid; **AD** = Alzheimer disease; **CDR** = Clinical Dementia Rating; **CDR-SB** = Clinical Dementia Rating scale, Sum of Boxes; **CI** = confidence interval; **FTP** = flortaucipir; **FWE** = familywise error; **GLM** = General Linear Model; **GM** = gray matter; **LBNL** = Lawrence Berkeley National Laboratory; **lvPPA** = logopenic variant primary progressive aphasia; **MTL** = medial temporal lobe; **PCA** = posterior cortical atrophy; **PiB** = Pittsburgh compound B; **PVC** = partial volume correction; **SUVR** = standard uptake value ratio; **UCSF** = University of California San Francisco; **VBM** = voxel-based morphometry.

The clinical expression of Alzheimer disease (AD) is heterogeneous and expands beyond the traditionally described older age amnestic dementia syndrome.[1–3] First, age at symptom onset is highly variable; whereas the incidence of AD dementia increases with age,[4] ~5% of patients with sporadic AD develop symptoms before age 65.[5] The ε4 allele of *APOE* (*APOE4*) is associated with an earlier disease onset.[3] Second, memory loss is a frequent but inconsistent presenting feature of AD such that evidence of memory impairment is no longer required for the diagnosis of probable AD dementia.[6] Nonamnestic AD phenotypes have been well characterized: visuospatial-predominant posterior cortical atrophy (PCA)[7] and language-predominant logopenic variant primary progressive aphasia (lvPPA).[8] These atypical variants tend to have an early age at onset, but they are associated with a relatively low frequency of *APOE4*.[3] Establishing the relationships between clinical variability and the key pathophysiologic processes in AD, β-amyloid (Aβ), and tau, and neurodegeneration, could inform our understanding of mechanisms driving disease heterogeneity.

We aimed to determine the molecular pathology correlates of phenotypic variant, age at onset, and *APOE4* in patients at symptomatic stages of AD, using PET to quantify Aβ and tau. Based on previous case series[9–11] and autopsy studies,[12,13] we expected that the distribution of tau, not Aβ, would mirror cognitive phenotypes. We also expected tau burden to be higher in younger patients,[9,14] but investigated whether this relationship was driven by the higher frequency of atypical variants at younger ages or whether it existed across phenotypes. Finally, we expected *APOE4* to be associated with a more medial temporal lobe (MTL)–predominant pattern,[3] especially for tau pathology.[15,16]

Methods

Patients

This retrospective study included patients recruited from the University of California San Francisco (UCSF) Alzheimer Disease Research Center. All patients underwent a comprehensive clinical evaluation including medical, physical examination, a structured caregiver interview, and neuropsychological testing. Clinical diagnosis was established by consensus in a multidisciplinary conference blinded to CSF or PET biomarker results.

For this study, we selected patients who fulfilled the following criteria: (1) clinical diagnosis of mild cognitive impairment or dementia due to AD based on the National Institute on Aging–Alzheimer's Association 2011 criteria,[6,17] (2) available 3T-MRI and PET with both [^{11}C] Pittsburgh compound B (PiB) for amyloid and [^{18}F] flortaucipir (FTP) for tau, and (3) PiB-PET read as positive based on both visual read and image quantification (see below). Patients with a known pathogenic mutation in *APP/PSEN1/PSEN2* were excluded.

As of July 15, 2020, 119 patients fulfilled these criteria, including 29 patients who also fulfilled criteria for lvPPA[8] and 21 patients who fulfilled criteria for PCA[7] at the time of enrollment into our study. The remaining 69 patients are simply referred to as having AD as they did not fulfill additional existing diagnostic criteria for an AD subtype at the time of their clinical visit. Based on this definition by default, this latter group is expected to be more clinically heterogeneous than the other 2 and to include a mix of patients with various types of presentations: some with prominent memory deficits, some with a more dysexecutive presentation,[18,19] some with no clear predominant cognitive pattern.

A total of 49/119 patients (39%) were at the mild or moderate stage of dementia, based on a Clinical Dementia Rating (CDR) score of 1 (n = 47) or 2 (n = 3). Demographics are available in table 1.

Standard Protocol Approvals, Registrations, and Patient Consents

Written informed consent was obtained from all patients or their surrogates. The study was approved by the institutional review boards at UCSF, University of California Berkeley, and Lawrence Berkeley National Laboratory (LBNL).

Imaging Acquisition

Patients underwent 3T MRI at UCSF on either a 3T Siemens Tim Trio (n = 37) or a 3T Siemens Prisma Fit (n = 82) scanner. T1-weighted magnetization prepared rapid gradient echo MRI sequences were used in the present study (sagittal slice orientation; 1 × 1 × 1 mm resolution; slices per slab = 160; matrix = 240 × 256; repetition time = 2.3 ms; inversion time = 900 ms; flip angle = 9°; echo time = 2.98 ms for Trio, 1.9 for Prisma).

PET scanning was performed at the LBNL on a Siemens Biograph PET/CT scanner. Radiotracers were synthesized and radiolabeled at LBNL's Biomedical Isotope Facility. We analyzed PET data that were acquired from 50 to 70 minutes after the injection of ~15 mCi of PiB (four 5-minute frames)

Table 1 Demographics and Cognitive Scores

	AD (n = 69)	PCA (n = 21)	lvPPA (n = 29)	Significance
Age, y	66.9 ± 10.0	62.5 ± 7.7	63.5 ± 8.1	$\eta^2 = 0.04$, $p = 0.08$
Female	36 (52%)	12 (57%)	14 (48%)	V = 0.06, $p = 0.83$
Years of education	16.8 ± 2.4	16.0 ± 3.3	17.7 ± 2.6	$\eta^2 = 0.05$, $p = 0.07$
Right-handedness	58 (84%)	17 (81%)	26 (90%)	V = 0.08, $p = 0.67$
***APOE4* carriers**	38 (64%); n = 59	8 (44%); n = 18	13 (57%); n = 23	V = 0.15, $p = 0.31$
MMSE (/30)	22.4 ± 5.8	21.2 ± 4.7	21.0 ± 6.0	$\eta^2 = 0.01$, $p = 0.47$
CDR-SB (/18)	4.1 ± 2.2	4.4 ± 2.4	3.3 ± 1.8	$\eta^2 = 0.03$, $p = 0.15$
CVLT: total immediate recall (/36)	19 ± 6.0; n = 63	17.7 ± 6.6; n = 18	15.0 ± 7.1; n = 26	$\eta^2 = 0.06$, $p = 0.03$ AD > lvPPA*
CVLT: 10 minutes recall (/9)	2.0 ± 2.5; n = 63	3.6 ± 2.6; n = 18	3.0 ± 3.1; n = 26	$\eta^2 = 0.06$, $p = 0.045$ AD < PCA,† AD < lvPPA‡
CVLT: forgetting[a]	3.7 ± 2.3; n = 63	1.8 ± 2.0; n = 18	1.7 ± 1.2; n = 26	$\eta^2 = 0.18$, $p < 0.001$ AD > PCA,§ AD > lvPPA§
Benson figure, copy (/17)	13.1 ± 4.2; n = 68	5.4 ± 4.3; n = 19	14.1 ± 3.8; n = 29	$\eta^2 = 0.35$, $p < 0.001$ PCA < AD,§ PCA < lvPPA§
Benson figure, 10 minutes recall (/17)	4.3 ± 3.7; n = 67	3.4 ± 3.8; n = 18	6.7 ± 4.4; n = 29	$\eta^2 = 0.09$, $p = 0.007$ AD < lvPPA,* PCA < lvPPA*
Benson figure forgetting[a]	8.8 ± 4.8; n = 67	1.9 ± 2.3; n = 18	7.4 ± 4.6; n = 29	$\eta^2 = 0.23$, $p < 0.001$ AD > PCA,§ lvPPA > PCA§
Boston Naming Test, correct (/15)	12.4 ± 3.3; n = 67	10.1 ± 3.8; n = 18	10.1 ± 4.0; n = 29	$\eta^2 = 0.09$, $p = 0.004$ PCA < AD,† lvPPA < AD*
Verbal fluency (letter D), 1 min	11.0 ± 5.3; n = 66	11.4 ± 6.0; n = 19	9.4 ± 5.7; n = 28	$\eta^2 = 0.02$, $p = 0.35$
Verbal fluency (animals), 1 min	12.5 ± 5.9; n = 64	10.8 ± 5.9; n = 20	10.3 ± 6.5; n = 28	$\eta^2 = 0.03$, $p = 0.22$
DKEFS Design Fluency, 1 min	6.5 ± 3.6; n = 64	2.9 ± 1.8; n = 15	6.7 ± 2.5; n = 25	$\eta^2 = 0.15$, $p < 0.001$ PCA < AD,§ PCA < lvPPA§
Sentence repetition (/5)	4.2 ± 1.2; n = 64	3.6 ± 1.4; n = 21	2.0 ± 1.3; n = 29	$\eta^2 = 0.37$, $p < 0.001$ lvPPA < AD,§ lvPPA < PCA,§ PCA < AD†
Modified Trail Making Test, time	70.0 ± 40.6; n = 55	101 ± 26.6; n = 10	81.4 ± 38.2; n = 25	$\eta^2 = 0.06$, $p = 0.06$
Stroop color naming, correct, 1 min	56.6 ± 22.3; n = 60	40.2 ± 20; n = 13	38.0 ± 19.9; n = 25	$\eta^2 = 0.15$, $p < 0.001$ PCA < AD,† lvPPA < AD§
Stroop interference, correct, 1 min	27.3 ± 16.2; n = 52	17.4 ± 12.6; n = 11	15.1 ± 12; n = 21	$\eta^2 = 0.13$, $p = 0.004$ PCA < AD,† lvPPA < AD*
Digit span forward, length	6.0 ± 1.3; n = 68	5.6 ± 1.1; n = 21	4.3 ± 0.8; n = 28	$\eta^2 = 0.28$, $p < 0.001$ lvPPA < AD,§ lvPPA < PCA§
Digit span backward, length	4.0 ± 1.6; n = 68	3.2 ± 1.3; n = 21	3.4 ± 0.9; n = 26	$\eta^2 = 0.06$, $p = 0.04$ PCA < AD,† lvPPA < AD‡
VOSP number location, correct (/10)	7.5 ± 2.5; n = 61	5.3 ± 2.9; n = 12	8.0 ± 2.3; n = 23	$\eta^2 = 0.09$, $p = 0.01$ PCA < AD,* PCA < lvPPA*
Geriatric Depression Scale (/30)	7.3 ± 5.2; n = 61	7.9 ± 4.9; n = 18	7.2 ± 4.2; n = 25	$\eta^2 < 0.01$, $p = 0.85$

Abbreviations: AD = typical Alzheimer disease; CDR-SB = Clinical Dementia Rating scale, Sum of Boxes; CVLT = California Verbal Learning Test (second edition, short form); DKEFS = Delis-Kaplan Executive Function System (condition 1); lvPPA = logopenic variant primary progressive aphasia; MMSE = Mini-Mental State Examination; PCA = posterior cortical atrophy; VOSP = Visual Object and Space Perception battery.
Data shown as mean ± SD for continuous variables or n (%) for categorical variables; for variables with missing data, the number of available values is indicated. Group comparisons were run using one-way analyses of variance or χ^2 tests; effect sizes (η^2 or Cramer V, respectively) are provided. When $p < 0.05$, post hoc tests were conducted, and significant contrasts are reported (*$p < 0.01$, †$p < 0.05$, ‡$p < 0.1$, §$p < 0.001$).
[a] For the 2 memory tests, forgetting scores were created; higher scores reflect more severe forgetting over time. For CVLT: number of recalled items on 4th learning trial minus number of recalled items on 10-minute delayed recall; for Rey figure: copy score minus 10-minute delayed recall score.

and 80–100 minutes after the injection of ~10 mCi of FTP (four 5-minute frames). A low-dose CT scan was performed for attenuation correction prior to PET acquisition, and PET data were reconstructed using an ordered subset expectation maximization algorithm with weighted attenuation and scatter correction; a 4-mm Gaussian smoothing kernel was applied during reconstruction (image resolution: 6.5 × 6.5 × 7.25 mm estimated based on Hoffman phantom).

Imaging Processing

Image processing was performed as previously described.[20] T1 MRIs were segmented using Freesurfer version 5.3 (surfer.nmr.mgh.harvard) and warped with Statistical Parametric Mapping 12 (Wellcome Department of Imaging Neuroscience, Institute of Neurology, London, UK). PET frames were realigned, averaged, and coregistered onto their corresponding MRI. Standard uptake value ratios (SUVRs) were created using tracer-specific reference regions: cerebellar gray matter (GM) for PiB and inferior cerebellar GM for FTP. PiB scans were visually read as positive or negative.[20]

To obtain a measure of global cortical Aβ and tau burden, we extracted a mean cortical SUVR value for each tracer in native space using a weighted average of all Freesurfer-derived cortical regions. For volumetric analyses (i.e., voxel-based morphometry), GM segments were warped to template, modulated, and smoothed using an 8-mm isotropic Gaussian kernel. SUVR maps were also warped to template space using SPM12 and the parameters defined from the MRI procedure to conduct voxelwise analyses. Warped SUVR images were masked with the intracranial mask and smoothed with a 4-mm isotropic Gaussian kernel[20] to reach final 8 mm^3 and match MRI resolution. This masking step was meant to limit contamination from nonrelevant areas (e.g., off-target binding from meninges or skull).

Unless otherwise specified, PET values presented in this manuscript are not corrected for partial volume effects. For some confirmatory analyses, we used data that were corrected using a method based on the geometric transfer matrix approach and tailored for FTP-PET.[21]

Statistical Analyses

We first aimed to test the association between (1) global cortical burden of Aβ and tau and (2) clinical variables, including patient age, disease severity (measured using the CDR Sum of Boxes [CDR-SB]), and phenotype (3 levels: AD, lvPPA, PCA). We first explored these associations using bivariate Pearson correlations and Welch 1-way analyses of variance. Then, a General Linear Model (GLM) was run for each tracer using the cortical SUVR as the dependent variable and age, CDR-SB, and phenotype as independent variables. Subsequent models were run adding an age*phenotype interaction, to test whether the expected relationship between tau and age differed between phenotypes. Finally, the main models (without the age*phenotype interaction) were re-run, adding *APOE* genotype as an independent variable (coded as positive or negative for the ε4 allele) on the subset of patients with available *APOE* data (n = 100 due to missing values).

Voxelwise analyses were run in SPM12 to assess relationships between clinical features and the regional distribution of PiB, FTP, and GM volume. For PiB and FTP, GLMs were conducted in every cortical GM voxel with age, CDR-SB, phenotype, and global cortical SUVR as independent variables. The latter was introduced in the models comparing phenotypes due to our interest in studying the relative distribution of pathology regardless of the absolute amount. When comparing GM volume between phenotypes using voxel-based morphometry (VBM), the global GM volume was introduced as a covariate instead of global cortical SUVR.

Voxelwise analyses were thresholded using 2 approaches. First, a relatively liberal threshold consisted of an uncorrected $p < 0.001$ at the voxel level combined with a familywise error (FWE)–corrected $p < 0.05$ at the cluster level using the CAT12 toolbox (neuro.uni-jena.de/cat/). Second, a more stringent $p_{FWE} < 0.05$ voxel level threshold was applied. When displaying associations between voxelwise SUVR values and age, SPM T-maps were converted to correlation coefficient maps using CAT12. For the sake of visualization, all voxel-based maps derived from PET and VBM analyses were rendered on a 3D brain surface using the BrainNet Viewer software (nitrc.org/projects/bnv/). Moreover, volumes corresponding to all group-level voxel-wise figures are freely available for viewing or download on neurovault, including thresholded and nonthresholded images (neurovault.org/collections/WMNXGOCS/).

Data Availability

Data are available upon request (memory.ucsf.edu/research-trials/professional/open-science).

Results

The patients included in the current study covered a large age range (48–95 years old, mean 65.3, SD 9.3), 52% female, and had all completed at least a high school education (table 1). A total of 96% of the patients were White. Phenotypic groups were comparable on demographics, *APOE4* genotype, or global clinical measures, i.e., MMSE and CDR-SB, but clear differences emerged when looking at specific cognitive tests (table 1). As expected, the PCA group had marked deficits on all visuospatial tests (figure copy, design fluency, modified Trail-Making Test, number location), while the lvPPA group had major deficits in verbal tests, especially those involving phonologic short-term memory (learning trials for the California Verbal Learning Test, sentence repetition, Digit Span Forward). The AD group showed lower delayed memory scores than the other phenotypes, with marked forgetting of both verbal and visual items over a 10-minute period.

Clinical Correlates of Global Aβ and Tau Burden

Global cortical PiB uptake was not related to any clinical variable (see figure 1 for univariate analyses and table 2 for GLMs).

Figure 1 Relationships Between Global Cortical PET Standard Uptake Value Ratio (SUVR) Values and Clinical Variables: Univariate Analyses

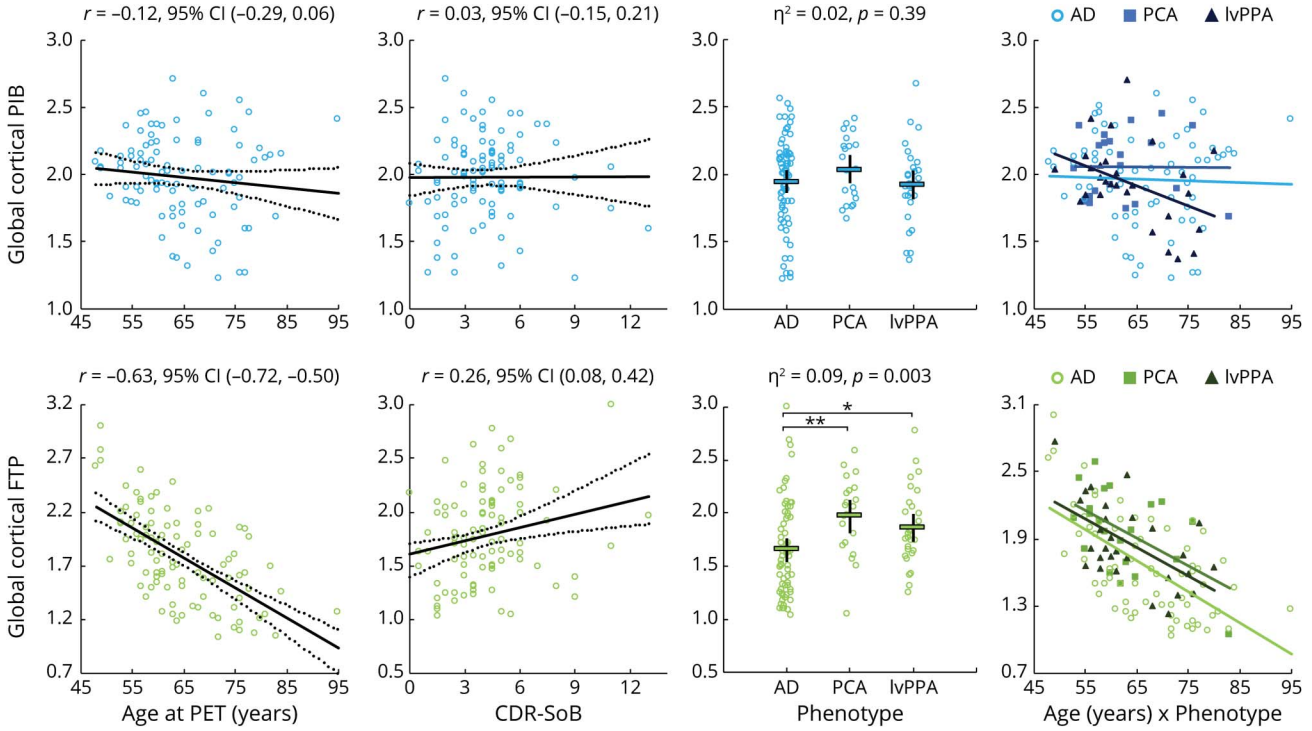

All data are raw, i.e., not adjusting for other variables, and statistics correspond to simple (univariate) models; see text and table 2 for general linear models with multiple variables. Regression plots are shown with regression line (dark line) and 95% confidence interval (CI) (dotted lines). Dotplots show average values (thick black bar) and 95% CI (thinner bars). *Mean difference = 0.210, 95% CI (0.030, 0.390), $p = 0.02$; **mean difference = 0.316, 95% CI (0.113, 0.519), $p = 0.003$; logopenic variant primary progressive aphasia (lvPPA)–posterior cortical atrophy (PCA) mean difference = 0.106 (−0.127, 0.340), $p = 0.37$. Plots in the rightmost column illustrate relationships between age and SUVR values, with regression lines calculated for each phenotype separately; see Results section for details. AD = Alzheimer disease; CDR-SB = Clinical Dementia Rating scale, Sum of Boxes; FTP = flortaucipir; PiB = Pittsburgh compound B.

The full model including age, CDR-SB, and phenotype as independent predictors only explained 2.8% of PiB SUVR variance and was not significant ($F_{4,114} = 0.82$, $p = 0.52$). The added phenotype*age interaction term was not significant ($p = 0.24$, $\eta^2 = 0.025$; see figure 1 to visualize age–PiB relationships within each phenotype separately). Similarly, *APOE4* was not associated with PiB SUVR ($p = 0.50$, $\eta^2 = 0.005$, table 2).

In contrast, global FTP was associated with all 3 clinical variables (figure 1, bottom row). In the GLM, the 3 clinical predictors were independently associated with FTP, altogether accounting for 48.0% of total variance ($F_{4,114} = 26.3$, $p < 0.001$). SUVR values decreased with patient age and increased with CDR-SB (see table 2 for specific estimates). In the same model, cortical FTP varied across phenotypes ($F = 4.1$, $p = 0.02$, $\eta^2 = 0.067$) and post hoc analyses showed that both lvPPA and PCA had higher FTP-SUVR than AD (see table 2). Adding a phenotype*age interaction term showed that the relationship between increasing age and lower FTP did not differ across phenotypes ($p = 0.86$, $\eta^2 = 0.003$). Inverse associations between age and FTP can be seen within each phenotype group in figure 1, showing very similar age–FTP slopes: −0.028 (−0.036, −0.019) for AD, −0.025 (−0.044, −0.005) for PCA, and −0.025 (−0.040, −0.011) for lvPPA. *APOE4* was not associated with global cortical FTP ($p = 0.69$, $\eta^2 = 0.002$, table 2).

Voxelwise Analyses

Phenotypes

The regional distribution of PiB and FTP across phenotypes is shown in figure 2.

PiB (figure 2A, top) was distributed throughout the cortex, especially in medial areas (medial prefrontal areas, posterior cingulate, and precuneus), lateral frontal, and temporoparietal cortices. PiB patterns were mostly similar across phenotypes (figure 2B, top), although the PCA group had slightly elevated SUVR values in the right medial occipital area compared to the other variants and the AD group showed slightly elevated PiB values in the left middle and inferior temporal gyri. However, none of these contrasts survived stringent FWE correction for multiple comparisons.

The pattern of elevated FTP (figure 2A, bottom) was more restricted than PiB. All groups had high FTP SUVR values in the temporoparietal and dorsolateral frontal areas with relative preservation of the sensorimotor and medial prefrontal cortex. FTP patterns showed strong between-phenotype variations, all contrasts being significant at $p_{FWE} < 0.05$ at the voxel level (figure 2B, bottom). The PCA group had higher bilateral occipital and to a lesser extent right parietal SUVR

Table 2 Relationships Between Clinical Measures and Global Cortical PET Measures

	Full sample (n = 119)		*APOE* sample (n = 100)	
	Estimate (95% CI)	Standardized estimates	Estimate (95% CI)	Standardized estimates
Dependent variable: cortical PiB				
Intercept	1.971 (1.894, 2.047)	—	1.965 (1.85, 2.08)	—
Age	−0.004 (−0.010, 0.003)	−0.110	−0.003 (−0.009, 0.004)	−0.085
CDR-SB	0.000 (-0.027, 0.028)	0.003	0.003 (-0.028, 0.033)	0.019
PCA	0.077 (−0.082, 0.236)	0.244	0.056 (−0.115, 0.226)	0.183
lvPPA	−0.039 (−0.181, 0.103)	−0.123	−0.047 (−0.201, 0.107)	−0.154
APOE4	—	—	0.043 (−0.083, 0.170)	0.142
Dependent variable: cortical FTP				
Intercept	1.687 (1.612, 1.763)	—	1.672 (1.553, 1.791)	—
Age	−0.026 (−0.033, −0.02)	−0.573	−0.027 (−0.034, −0.02)	−0.582
CDR-SB	0.047 (0.02, 0.074)	0.238	0.040 (0.008, 0.071)	0.189
PCA	0.187 (0.03, 0.345)	0.438	0.181 (0.006, 0.357)	0.419
lvPPA	0.158 (0.017, 0.299)	0.369	0.187 (0.029, 0.346)	0.433
APOE4+	—	—	0.026 (-0.105, 0.157)	0.060

Abbreviations: AD = Alzheimer disease; CDR-SB = Clinical Dementia Rating scale, Sum of Boxes; CI = confidence interval; FTP = flortaucipir; lvPPA = logopenic variant primary progressive aphasia; PCA = posterior cortical atrophy; PiB = Pittsburgh compound B.
Results of 4 separate general linear models assessing the effect of age (in years), clinical severity (CDR-SB), clinical phenotype (coded as a 3-level categorical variable using the AD group as a reference), and *APOE4* status (coded as ε4 carriers vs noncarrier, using the latter as a reference) on global cortical amyloid- or tau-PET signal. Age and CDR-SB are mean-centered so that each model's intercept represents the model estimate for a patient with AD for age = 65.3 and CDR-SB = 4.0.

values. The lvPPA group had increased signal in the left perisylvian cortex, including superior and anterior temporal and frontal areas. The AD group had relatively increased FTP in the bilateral MTLs.

We also tested group differences in GM volumes using voxel-based morphometry. Results are presented in figure 3 and show patterns that were highly similar to the pattern of FTP differences (figure 2, bottom). The main difference is that the only small cluster of significantly lower volume in the AD group was located in the right orbito-frontal cortex, not in the MTL as observed with FTP-PET. However, further investigation of the voxelwise results showed differences in the bilateral MTL at a voxel-wise uncorrected threshold of $p < 0.001$; these group differences do not show on figure 3 because they did not survive the cluster-level correction we prespecified for this study (see nonthresholded map on neurovault).

Age

Voxelwise analyses were conducted to further assess the negative association between age and cortical FTP-SUVR (figure 1 and table 2) and test whether this effect was regionally distributed.

FTP-SUVR was strongly and negatively correlated with patient age in most of the frontal and parietal cortex (r values down to −0.7 in peak regions), including the posterior cingulate and precuneus regions (figure 4A). An additional voxelwise model showed no significant phenotype*age interaction on FTP SUVR, and figure 4B shows that negative age–FTP relationships existed in all phenotypic groups, mostly in frontal and parietal areas. Regions previously identified as particularly elevated in each phenotype (MTL in AD, left temporo-parietal in lvPPA, and occipital in PCA) showed minimal age effect in their respective group.

No positive association (i.e., higher FTP-SUVR values in older patients) was significant, even at the liberal ($p_{\text{uncorrected}} < 0.001$) threshold.

APOE4

Voxelwise analyses of the association between *APOE4* and PiB SUVR did not show any significant cluster, even at the liberal threshold.

In contrast, the presence of 1 or more ε4 alleles was associated with increased FTP SUVR in the bilateral MTLs, with voxels reaching $p_{\text{FWE}} < 0.05$ while controlling for age, phenotype, and CDR-SB (figure 5A). No cluster was significant in the reverse contrast.

Because of the focality of the significant cluster and due to the proximity of off-target binding sources (e.g., choroid plexus and extra-axial areas medial to the entorhinal cortex), we

Figure 2 Differences in the Regional Distribution of Pittsburgh Compound B (PiB) and Flortaucipir Across Alzheimer Disease (AD) Phenotypes

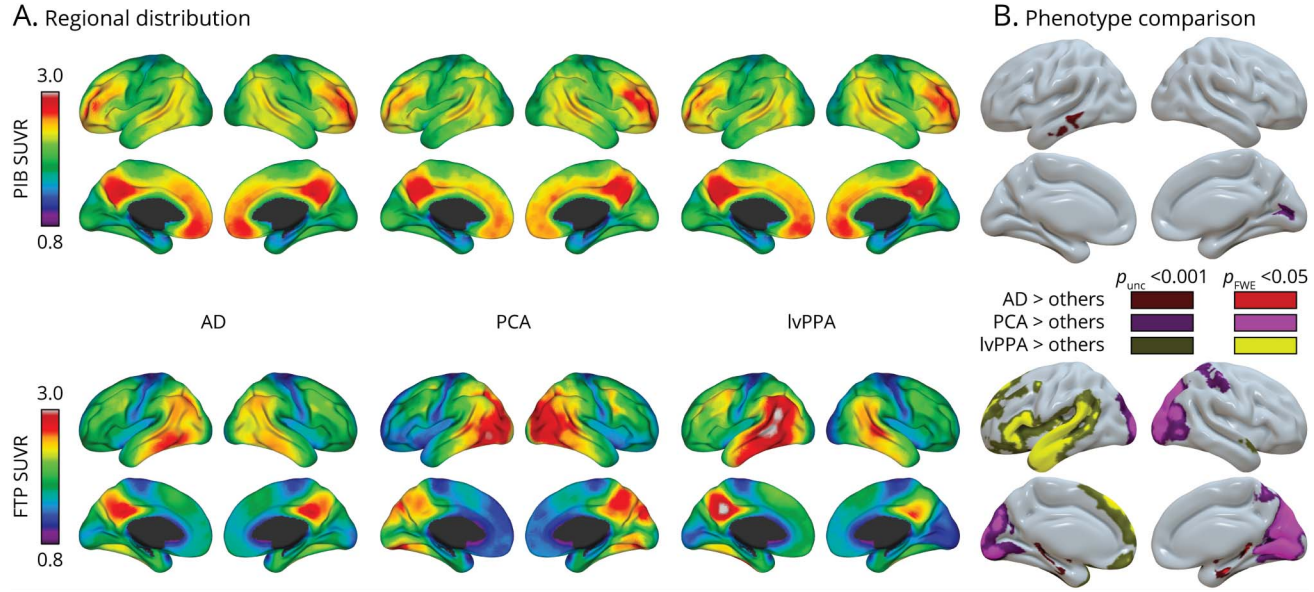

(A) The relative distributions of Pittsburgh compound B (PiB) (top) and flortaucipir (FTP) (bottom) within each phenotype. Maps show marginal means, i.e., predicted standard uptake value ratio (SUVR) values for the whole cohort's average age (65.3 years), Clinical Dementia Rating scale, Sum of Boxes (CDR-SB) (4.0), and global cortical SUVR. (B) Results of the voxelwise analysis of covariance testing for phenotype differences, controlling for age, CDR-SB, and global cortical PiB/FTP SUVR. Each group comparison is shown with a liberal (dark; unc: uncorrected) and stringent (bright; FWE: familywise error corrected) statistical threshold. All panels represent voxel-based images derived from Statistical Parametric Mapping 12 that were interpolated onto a brain surface using BrainNetViewer for visualization purposes. Corresponding unthresholded and thresholded 3D voxel-wise maps are available at neurovault (neurovault.org/collections/WMNXGOCS/). lvPPA = logopenic variant primary progressive aphasia; PCA = posterior cortical atrophy.

performed post hoc analyses using partial volume correction (PVC) in 2 bilateral Freesurfer-defined regions: the entorhinal cortex and amygdala.

Resulting mean entorhinal $SUVR_{PVC}$ were higher in direct comparison of *APOE4* carriers vs noncarriers with a 2-sample *t* test (difference = 0.348, 95% confidence interval [CI]

Figure 3 Gray Matter Volume Differences Between Phenotypes

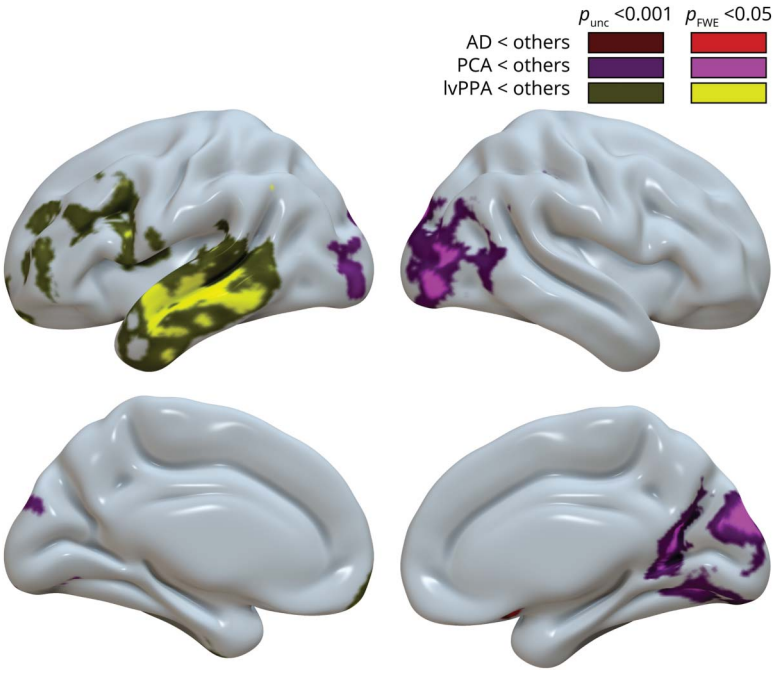

Results of the voxelwise analysis of covariance, testing for phenotype differences in gray matter volume, controlling for age, Clinical Dementia Rating scale, Sum of Boxes, and global cortical gray matter volume. Each group comparison is shown with a liberal (dark; unc: uncorrected) and stringent (bright; FWE: familywise error corrected) statistical threshold. The figure illustrates voxel-based results obtained with Statistical Parametric Mapping 12 that were interpolated onto a brain surface using BrainNetViewer for visualization purposes. Corresponding unthresholded and thresholded 3D voxelwise maps are available at neurovault (neurovault.org/collections/WMNXGOCS/). AD = Alzheimer disease; lvPPA = logopenic variant primary progressive aphasia; PCA = posterior cortical atrophy.

Figure 4 Relationships Between Patients' Age and Flortaucipir (FTP)–Standard Uptake Value Ratio (SUVR): Voxelwise Analyses

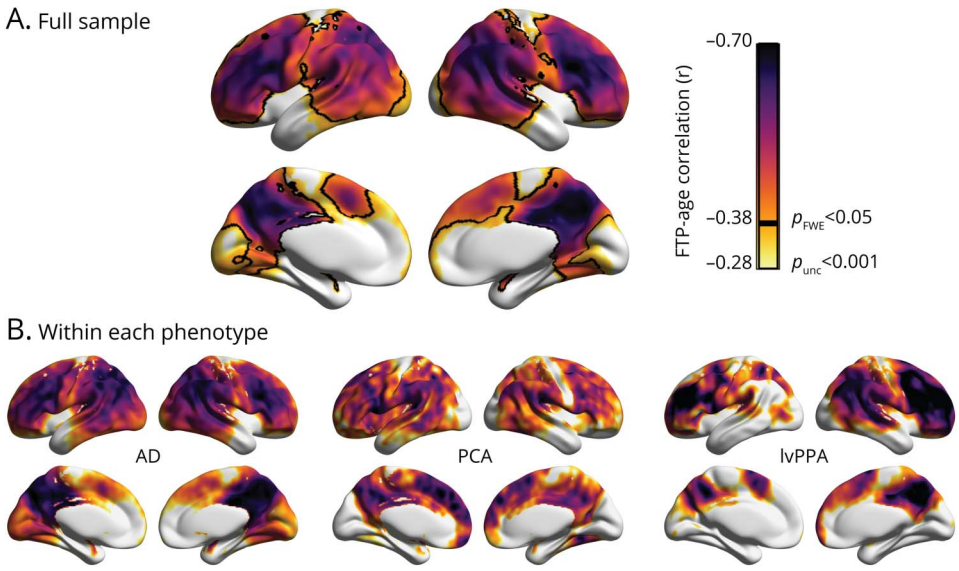

(A) Statistical model was run on the full sample (n = 119) and included disease severity (Clinical Dementia Rating scale, Sum of Boxes [CDR-SB], continuous variable) and phenotype (categorical variable, 3 levels) as covariates. Results were thresholded using $p_{uncorrected}$ < 0.001 at the voxel level (corresponding to r = −0.28) with p_{FWE} < 0.05 at the cluster level and expressed as correlation coefficients; a black line represents an r value of −0.38, which corresponds to a voxel-level p_{FWE} < 0.05 threshold in the full sample (n = 119). (B) Associations between age and flortaucipir standard uptake value ratio within each phenotype. Maps were obtained from 3 separate voxelwise models, each controlling for CDR-SB. Results were not thresholded using a p value to avoid bias due to different sample size and power, but shown using the same color scale as in panel A. All panels represent voxel-based images derived from Statistical Parametric Mapping 12 that were interpolated onto a brain surface using BrainNetViewer for visualization purposes. Corresponding unthresholded and thresholded 3D voxel-wise maps are available at neurovault (neurovault.org/collections/WMNXGOCS/). AD = Alzheimer disease; FWE = familywise error; lvPPA = logopenic variant primary progressive aphasia; PCA = posterior cortical atrophy; unc = uncorrected.

[0.127, 0.570], η^2 = 0.09; see figure 5B, green). Entorhinal FTP-SUVR$_{PVC}$ was then entered as the dependent variable of a GLM with age, phenotype, CDR-SB, and *APOE4* as predictors (figure 5B, gray). In the full model (F = 3.8, p = 0.004, R^2 = 0.17), the presence of *APOE4* was associated with higher entorhinal FTP-SUVR$_{PVC}$ values (difference = 0.310

Figure 5 *APOE4*-Associated Differences in Flortaucipir (FTP)–Standard Uptake Value Ratio (SUVR)

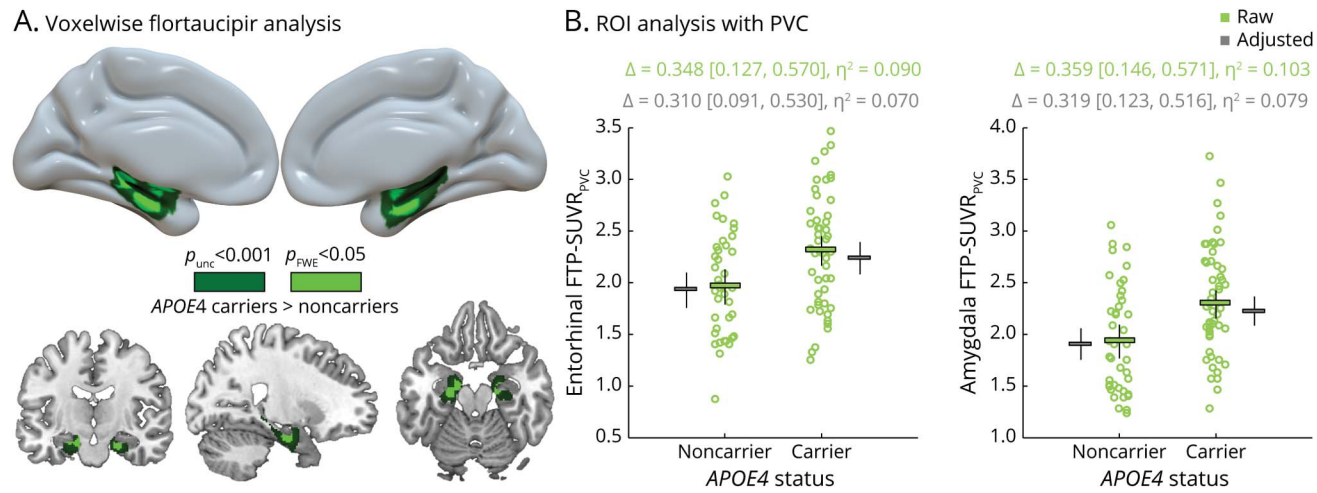

(A) Results of the voxelwise analysis of covariance testing for *APOE4* differences in flortaucipir SUVR, controlling for age, Clinical Dementia Rating scale, Sum of Boxes (CDR-SB), and phenotype, and shown with both a liberal (unc: uncorrected) and a stringent (FWE: familywise error corrected) statistical threshold; no significant clusters were found in the reverse contrast. Top panel represents a voxel-based analysis derived from Statistical Parametric Mapping 12 that was interpolated onto a brain surface using BrainNetViewer for visualization purposes. Lower panel shows significant clusters displayed on the ch2better template using MRICRON. Corresponding unthresholded and thresholded 3D voxelwise maps are available at neurovault (neurovault.org/collections/WMNXGOCS/). (B) Confirmatory region of interest (ROI) analyses using partial volume corrected (PVC) SUVR values extracted from the bilateral entorhinal cortex and amygdala. Plot shows raw data with mean values and 95% confidence interval (CI) in green and the estimated marginal means and 95% CI (controlling for age, CDR-SB and phenotype) in gray.

[0.091, 0.530], $\eta^2 = 0.07$), while higher CDR-SB ($p = 0.051$, $\eta^2 = 0.04$), phenotype ($p = 0.11$, $\eta^2 = 0.06$), and age ($p = 0.37$, $\eta^2 < 0.01$) had little to no effect. Finally, no phenotype*A-*POE4* interaction was observed on entorhinal $SUVR_{PVC}$ ($p = 0.55$, $\eta^2 = 0.01$) and the effect of *APOE4* on entorhinal FTP-$SUVR_{PVC}$ remained significant (difference = 0.408 [0.106, 0.709], $\eta^2 = 0.11$ controlling for age and CDR-SB) when restricting the analysis to the 59 cases from the AD group with available *APOE* genotype.

Results were comparable when testing the effect of *APOE4* on amygdala FTP-$SUVR_{PVC}$ (figure 5): *APOE4* carriers had higher FTP-$SUVR_{PVC}$ binding than noncarriers in a 2-sample *t* test (difference = 0.359, 95% CI [0.146, 0.571], $\eta^2 = 0.103$), and in a full model controlling for age, CDR-SB, and phenotype (difference = 0.319, 95% CI [0.123, 0.516], $\eta^2 = 0.079$). No phenotype**APOE4* was observed ($p = 0.35$, $\eta^2 = 0.02$), and the *APOE4*-related difference was observed in the AD group alone (difference = 0.440, 95% CI [0.182, 0.698], $\eta^2 = 0.134$, controlling for age and CDR-SB).

The effect of *APOE4* on medial temporal FTP-$SUVR_{PVC}$ remained unchanged when controlling for cortical PiB-SUVR in the models also including age, CDR-SB, and phenotype: mean *APOE4*-related FTP-$SUVR_{PVC}$ difference = 0.306 95% CI (0.085, 0.527) in the entorhinal cortex and 0.309 95% CI (0.113, 0.504) in the amygdala.

Discussion

There is a need to better characterize the heterogeneity of AD in order to develop precision medicine approaches for AD biomarker and drug discovery.[1,22] In the past decade, the variability of clinical and cognitive trajectories[2] or patterns of atrophy[23,24] has been highlighted in symptomatic patients with AD, but the neuropathologic underpinnings of this heterogeneity are not fully understood. Using PET imaging, we showed that Aβ pathology showed absent-to-weak correlations with clinical features, while the severity and regional distribution of tau was associated with age at onset, clinical severity, phenotype, atrophy patterns, and *APOE4*. While some of these associations were noted in previous articles, the size and heterogeneity of our cohort allowed us to look at these different factors all together.

Our finding that the pattern of tau, but not Aβ pathology, mirrors AD phenotype and atrophy patterns is in line with previous imaging reports[11,25–27] and neuropathologic investigations.[12,13] Although various studies have reported that Aβ is usually widespread and relates weakly to clinical and radiologic measures,[28,29] we did observe higher occipital Aβ load in the PCA group. This finding echoes a previous study from our laboratory on a nonoverlapping patient group[30] and an independent laboratory[31] while other studies have failed to replicate this effect.[32] In contrast to Aβ, tau distribution showed strong phenotype differences, consistent with well-described correlations between patterns of tau-PET and cognitive deficits.[33] Yet, over and above differences, tau-PET patterns clearly overlapped across phenotypes with the involvement of the inferolateral temporal cortex, lateral parietal, and posterior cingulate/precuneus areas in all groups. This temporoparietal tau-PET signal appears as the core AD signature common to most symptomatic patients with AD, while additional features (e.g., occipital tau in PCA, left predominant pattern in lvPPA) seem to account for atypical clinical presentations.

Curiously, we observed a phenotype-related difference where both atypical variants exhibited greater global cortical tau burden compared to the other patients with AD (similar to a small imaging case series[31] and a neuropathology study[13]), even when controlling for age and CDR-SB. This difference may reflect the limitations of CDR-SB as an index for disease severity across all patients (e.g., if CDR-SB is more sensitive to atypical amnestic symptoms), potentially resulting in a residual confounding issue when comparing atypical to typical variants. Alternatively, there might be actual differences in the disease pathophysiology between typical and atypical AD, either due to the involvement of different molecular Aβ or tau species[34] or differences in premorbid brain properties that could lead to a more rapid accumulation of pathology. For instance, lvPPA and PCA have been associated with a higher prevalence of developmental differences[35,36]; future studies are needed to understand how these might affect later-life pathology.

As previously reported,[9,14] we showed a strong relationship between patient age and global cortical tau-PET signal, with an average 0.026 SUVR unit decrease per year. This effect was mainly found in parietal and dorsolateral frontal cortices, and this phenomenon was observed across AD phenotypes, as suggested by a recent study.[37] The inverse correlation does not mean that tau burden decreases with disease progression: longitudinal FTP studies have shown PET signal increases over time, especially in symptomatic patients.[38] Instead, the age–FTP correlation could reflect secular cohort differences between early- vs late-onset AD, with younger patients being able to tolerate higher pathology burden than older patients while functioning at the same level, i.e., having higher resilience.[39] The association between age and tau-PET could also be related to different neuropathologic underpinnings between early- and late-onset AD, with the involvement of different molecular forms of tau.[40,41] In addition, late-onset AD dementia tends to be associated with mixed etiology, where multiple pathologies contribute to neurodegeneration and cognitive decline,[42] while patients with early-onset AD typically have more isolated or pure AD pathology.[43] Because of the lack of major age-related copathologies, younger patients could be able to tolerate higher levels of tau pathology before reaching the clinical stage of AD, explaining the cross-sectional correlation we observed between age and tau. The development of biomarkers for age-related copathologies will be needed to test this hypothesis.

In our cohort, *APOE4* had a very specific and focal effect on tau distribution in the MTL, and was unrelated to Aβ burden or

distribution. While the existence of an amyloid-independent *APOE4* effect on tau-PET is controversial,[16,44] our result replicates recent observations from a multi PET tracer study spanning cognitively normal controls and impaired patients with more typical AD presentations,[15] and shows that the *APOE4* effect on MTL tau is robust and does not depend on clinical characteristics. While a vast literature shows that *APOE4* is associated with an increased likelihood of Aβ positivity and an earlier onset of Aβ accumulation,[45] our data are in line with recent evidence that *APOE4* does not affect the later stages of the amyloidosis process.[46] Our results support the hypothesis of a pleiotropic effect of *APOE4* in AD pathophysiology, including amyloid-independent pathways[47] that exacerbate tau pathology, as observed from human-induced pluripotent stem cells[48] or in Aβ pathology–free rodent models.[49]

Interestingly, older age at onset and presence of *APOE4*, the 2 main risk factors for sporadic AD, appeared to have a comparable effect on the distribution of tau pathology: both factors resulted in a more limbic predominant[12] pattern, characterized by a higher MTL/cortical tau ratio.[16] Altogether, this indicates that clinical studies selecting participants based on older age and *APOE4* positivity are automatically enriched in typical, MTL-predominant pattern of tau deposition. This finding has implications for future AD clinical trials and observational studies, as any tau-PET–based measure of interest should be tailored to the demographic, genetic, and phenotypic characteristics of the cohort.

The present findings should be interpreted in light of the limitations of our cohort and study design. First, the current analyses were not conducted on a representative AD patient sample: our cohort was intentionally enriched for patients with nonamnestic phenotypes and individuals across a wide age range (i.e., extreme cases of the AD clinical spectrum) to encompass a large scope of AD clinical heterogeneity. However, other atypical phenotypes such as behavioral-dysexecutive AD[18,19] or corticobasal syndrome were not included in the present study. In contrast to the clinical heterogeneity, our cohort lacked diversity in terms of race/ethnicity and socioeconomic status, which also limits the generalizability of our findings. The cohort was highly educated, which may affect the association between pathology and brain atrophy or symptoms due to higher resilience.[39] Future studies are warranted to assess potential interactions between race/ethnicity and *APOE4*, as suggested by epidemiologic studies.[50] In addition, our results are based on cross-sectional data so we could not track the dynamics of neuroimaging changes over time. Longitudinal data will be needed to test whether atypical AD is associated with a more aggressive biological process (e.g., higher rates of tau burden increase) than typical AD.

We showed that atypical AD phenotypes share various features with typical AD: (1) widespread cortical Aβ deposition, (2) tau pathology in the temporo-parietal areas, and (3) higher tau burden associated with earlier disease onset. The main between-phenotype differences were variations in the distribution of tau, which mirrored differences in cortical atrophy. Our data also showed that the 2 main risk factors for sporadic AD (older age and *APOE4*) affect disease expression by promoting a more MTL-predominant pattern of tau pathology.

Acknowledgment

The authors thank the patients and families for their commitment and Elena Tsoy for her discussion on neuropsychological tests and figures. Avid Radiopharmaceuticals enabled the use of flortaucipir, but did not provide direct funding and were not involved in data analysis or interpretation.

Study Funding

The study was supported by NIH/National Institute of Aging grants P50-AG23501 (to G.D.R., B.L.M.), P30-AG062422 (to B.L.M., G.D.R.), P01-AG019724 (to B.L.M.), R01-AG045611 (to G.D.R.), R01-AG034570 (to W.J.J.), and K99AG065501 (to R.L.J.); Rainwater Charitable Foundation (to G.D.R., W.J.J.); and Alzheimer's Association (AARF:16-443577 [to R.L.J.] and AACSF:19-617663 [to D.S.M.]).

Disclosure

Dr. La Joie, A.V. Visani, Dr. Lesman-Segev, L. Edwards, Dr. Iaccarino, Dr. Soleimani-Meigooni, T. Mellinger, Dr. Janabi, Dr. Z.A. Miller, Dr. Perry, J. Pham, A. Strom, Dr. Gorno-Tempini, and Dr. Rosen have nothing to disclose. Dr. Baker consults for Genentech. Dr. B.L. Miller receives research support from the NIH/National Institute of Aging and the Centers for Medicare & Medicaid Services as grants for the Memory and Aging Center; and serves as Medical Director for the John Douglas French Foundation, Scientific Director for the Tau Consortium, Director/Medical Advisory Board of the Larry L. Hillblom Foundation, Scientific Advisory Board Member for the National Institute for Health Research Cambridge Biomedical Research Centre and its subunit, the Biomedical Research Unit in Dementia (UK), and Board Member for the American Brain Foundation (ABF). Dr. Jagust has served as a consultant to BioClinica, Genentech, and Novartis Pharmaceuticals. Dr. Rabinovici receives research support from Avid Radiopharmaceuticals, GE Healthcare, and Life Molecular Imaging; has received consulting fees or speaking honoraria from Axon Neurosciences, Avid Radiopharmaceuticals, GE Healthcare, Johnson & Johnson, Roche, Eisai, Genentech, and Merck; and is an associate editor of *JAMA Neurology*. Go to Neurology.org/N for full disclosures.

Publication History

Received by *Neurology* March 23, 2020. Accepted in final form September 11, 2020.

Appendix Authors

Name	Location	Contribution
Renaud La Joie, PhD	University of California, San Francisco	Designed and conceptualized study, analyzed and interpreted the data, drafted the manuscript

Continued

Appendix *(continued)*

Name	Location	Contribution
Adrienne V. Visani, BS	University of California, San Francisco	Analyzed and interpreted the data, revised the manuscript for intellectual content
Orit Lesman-Segev, MD	University of California, San Francisco	Analyzed and interpreted the data, revised the manuscript for intellectual content
Suzanne L. Baker, PhD	Lawrence Berkeley National Laboratory	Analyzed and interpreted the data, revised the manuscript for intellectual content
Lauren Edwards, BS,	University of California, San Francisco	Analyzed and interpreted the data, revised the manuscript for intellectual content
Leonardo Iaccarino, PhD	University of California, San Francisco	Analyzed and interpreted the data, revised the manuscript for intellectual content
David Soleimani-Meigooni, MD	University of California, San Francisco	Analyzed and interpreted the data, revised the manuscript for intellectual content
Taylor Mellinger, BS	University of California, San Francisco	Major role in the acquisition of data, revised the manuscript for intellectual content
Mustafa Janabi, PhD	Lawrence Berkeley National Laboratory	Major role in the acquisition of data, revised the manuscript for intellectual content
Zachary A Miller, MD	University of California, San Francisco	Major role in the acquisition of data, revised the manuscript for intellectual content
David C Perry, MD	University of California, San Francisco	Major role in the acquisition of data, revised the manuscript for intellectual content
Julie Pham, BA	University of California, San Francisco	Major role in the acquisition of data, revised the manuscript for intellectual content
Amelia Strom, BS	University of California, San Francisco	Analyzed and interpreted the data, revised the manuscript for intellectual content
Maria Luisa Gorno-Tempini, MD, PhD	University of California, San Francisco	Major role in the acquisition of data, revised the manuscript for intellectual content
Howard J. Rosen, MD	University of California, San Francisco	Major role in the acquisition of data, revised the manuscript for intellectual content
Bruce L. Miller, MD	University of California, San Francisco	Designed and conceptualized study, revised the manuscript for intellectual content
William J. Jagust, MD	University of California, Berkeley	Major role in the acquisition of data, revised the manuscript for intellectual content
Gil D. Rabinovici, MD	University of California, San Francisco	Designed and conceptualized study, major role in the acquisition of data, revised the manuscript for intellectual content

References

1. Devi G, Scheltens P. Heterogeneity of Alzheimer's disease: consequence for drug trials? Alzheimers Res Ther 2018;10:122.
2. Lam B, Masellis M, Freedman M, Stuss DT, Black SE. Clinical, imaging, and pathological heterogeneity of the Alzheimer's disease syndrome. Alzheimers Res Ther 2013;5:1.
3. van der Flier WM, Pijnenburg YA, Fox NC, Scheltens P. Early-onset versus late-onset Alzheimer's disease: the case of the missing APOE ε4 allele. Lancet Neurol 2011;10:280–288.
4. Reitz C, Brayne C, Mayeux R. Epidemiology of Alzheimer disease. Nat Rev Neurol 2011;7:137–152.
5. Zhu X-C, Tan L, Wang H-F, et al. Rate of early onset Alzheimer's disease: a systematic review and meta-analysis. Ann Transl Med 2015;3:38.
6. McKhann GM, Knopman DS, Chertkow H, et al. The diagnosis of dementia due to Alzheimer's disease: recommendations from the National Institute on Aging-Alzheimer's Association workgroups on diagnostic guidelines for Alzheimer's disease. Alzheimers Dement 2011;7:263–269.
7. Crutch SJ, Schott JM, Rabinovici GD, et al. Consensus classification of posterior cortical atrophy. Alzheimers Dement 2017;13:870–884.
8. Gorno-Tempini ML, Hillis AE, Weintraub S, et al. Classification of primary progressive aphasia and its variants. Neurology 2011;76:1006–1014.
9. Ossenkoppele R, Schonhaut DR, Schöll M, et al. Tau PET patterns mirror clinical and neuroanatomical variability in Alzheimer's disease. Brain 2016;139:1551–1567.
10. Phillips JS, Das SR, McMillan CT, et al. Tau PET imaging predicts cognition in atypical variants of Alzheimer's disease. Hum Brain Mapp 2018;39:691–708.
11. Nasrallah IM, Chen YJ, Hsieh MK, et al. ^{18}F-Flortaucipir PET-MRI correlations in non-amnestic and amnestic variants of Alzheimer disease. J Nucl Med 2018;59:299–306.
12. Murray ME, Graff-Radford NR, Ross OA, Petersen RC, Duara R, Dickson DW. Neuropathologically defined subtypes of Alzheimer's disease with distinct clinical characteristics: a retrospective study. Lancet Neurol 2011;10:785–796.
13. Petersen C, Nolan AL, de Paula França Resende E, et al. Alzheimer's disease clinical variants show distinct regional patterns of neurofibrillary tangle accumulation. Acta Neuropathol 2019;138:597–612.
14. Pontecorvo MJ, Devous MD, Navitsky M, et al. Relationships between flortaucipir PET tau binding and amyloid burden, clinical diagnosis, age and cognition. Brain J Neurol 2017;140:748–763.
15. Therriault J, Benedet AL, Pascoal TA, et al. Association of apolipoprotein E ε4 with medial temporal tau independent of amyloid-β. JAMA Neurol 2020;77:470–479.
16. Mattsson N, Ossenkoppele R, Smith R, et al. Greater tau load and reduced cortical thickness in APOE ε4-negative Alzheimer's disease: a cohort study. Alzheimers Res Ther 2018;10:77.
17. Albert MS, DeKosky ST, Dickson D, et al. The diagnosis of mild cognitive impairment due to Alzheimer's disease: recommendations from the National Institute on Aging-Alzheimer's Association workgroups on diagnostic guidelines for Alzheimer's disease. Alzheimers Dement 2011;7:270–279.
18. Ossenkoppele R, Pijnenburg YAL, Perry DC, et al. The behavioural/dysexecutive variant of Alzheimer's disease: clinical, neuroimaging and pathological features. Brain J Neurol 2015;138:2732–2749.
19. Townley RA, Graff-Radford J, Mantyh WG, et al. Progressive dysexecutive syndrome due to Alzheimer's disease: a description of 55 cases and comparison to other phenotypes. Brain Commun 2020;2:fcaa068.
20. La Joie R, Bejanin A, Fagan AM, et al. Associations between [18F]AV1451 tau PET and CSF measures of tau pathology in a clinical sample. Neurology 2018;90:e282–e290.
21. Baker SL, Maass A, Jagust WJ. Considerations and code for partial volume correcting [18F]-AV-1451 tau PET data. Data Brief 2017;15:648–657.
22. Khan SR, Manialawy Y, Wheeler MB, Cox BJ. Unbiased data analytic strategies to improve biomarker discovery in precision medicine. Drug Discov Today 2019;24:1735–1748.
23. Young AL, Marinescu RV, Oxtoby NP, et al. Uncovering the heterogeneity and temporal complexity of neurodegenerative diseases with subtype and stage inference. Nat Commun 2018;9:4273.
24. Ossenkoppele R, Cohn-Sheehy BI, La Joie R, et al. Atrophy patterns in early clinical stages across distinct phenotypes of Alzheimer's disease. Hum Brain Mapp 2015;36:4421–4437.
25. Xia C, Makaretz SJ, Caso C, et al. Association of in vivo [^{18}F]AV-1451 tau PET imaging results with cortical atrophy and symptoms in typical and atypical Alzheimer disease. JAMA Neurol 2017;74:427–436.
26. Cho H, Kim HJ, Choi JY, et al. ^{18}F-flortaucipir uptake patterns in clinical subtypes of primary progressive aphasia. Neurobiol Aging 2019;75:187–197.
27. Whitwell JL, Graff-Radford J, Tosakulwong N, et al. Imaging correlations of tau, amyloid, metabolism, and atrophy in typical and atypical Alzheimer's disease. Alzheimers Dement 2018;14:1005–1014.
28. La Joie R, Perrotin A, Barré L, et al. Region-specific hierarchy between atrophy, hypometabolism, and β-amyloid (Aβ) load in Alzheimer's disease dementia. J Neurosci Off J Soc Neurosci 2012;32:16265–16273.
29. Nelson PT, Alafuzoff I, Bigio EH, et al. Correlation of Alzheimer disease neuropathologic changes with cognitive status: a review of the literature. J Neuropathol Exp Neurol 2012;71:362–381.

30. Lehmann M, Ghosh PM, Madison C, et al. Diverging patterns of amyloid deposition and hypometabolism in clinical variants of probable Alzheimer's disease. Brain J Neurol 2013;136:844–858.
31. Day GS, Gordon BA, Jackson K, et al. Tau PET binding distinguishes patients with early-stage posterior cortical atrophy from amnestic Alzheimer disease dementia. Alzheimer Dis Assoc Disord 2017;31:87–93.
32. Beaufils E, Ribeiro MJ, Vierron E, et al. The pattern of brain amyloid load in posterior cortical Atrophy using 18F-AV45: is amyloid the principal actor in the disease? Dement Geriatr Cogn Disord Extra 2014;4:431–441.
33. Bejanin A, Schonhaut DR, La Joie R, et al. Tau pathology and neurodegeneration contribute to cognitive impairment in Alzheimer's disease. Brain J Neurol 2017;140: 3286–3300.
34. Qiang W, Yau W-M, Lu J-X, Collinge J, Tycko R. Structural variation in amyloid-β fibrils from Alzheimer's disease clinical subtypes. Nature 2017;541:217–221.
35. Miller ZA, Mandelli ML, Rankin KP, et al. Handedness and language learning disability differentially distribute in progressive aphasia variants. Brain J Neurol 2013; 136:3461–3473.
36. Miller ZA, Rosenberg L, Santos-Santos MA, et al. Prevalence of mathematical and visuospatial learning disabilities in patients with posterior cortical atrophy. JAMA Neurol 2018;75:728–737.
37. Whitwell JL, Martin P, Graff-Radford J, et al. The role of age on tau PET uptake and gray matter atrophy in atypical Alzheimer's disease. Alzheimers Dement 2019;15: 675–685.
38. Harrison TM, La Joie R, Maass A, et al. Longitudinal tau accumulation and atrophy in aging and Alzheimer disease. Ann Neurol 2019;85:229–240.
39. Arenaza-Urquijo EM, Vemuri P. Improving the resistance and resilience framework for aging and dementia studies. Alzheimers Res Ther 2020;12:41.
40. Aoyagi A, Condello C, Stöhr J, et al. Aβ and tau prion-like activities decline with longevity in the Alzheimer's disease human brain. Sci Transl Med 2019;11:eaat8462.
41. Dujardin S, Commins C, Lathuiliere A, et al. Tau molecular diversity contributes to clinical heterogeneity in Alzheimer's disease. Nat Med 2020;26:1256–1263.
42. Josephs KA, Dickson DW, Tosakulwong N, et al. Rates of hippocampal atrophy and presence of post-mortem TDP-43 in patients with Alzheimer's disease: a longitudinal retrospective study. Lancet Neurol 2017;16:917–924.
43. Gerritsen AAJ, Bakker C, Verhey FRJ, et al. Prevalence of comorbidity in patients with young-onset Alzheimer disease compared with late-onset: a comparative cohort study. J Am Med Dir Assoc 2016;17:318–323.
44. Ramanan VK, Castillo AM, Knopman DS, et al. Association of Apolipoprotein E ε4, educational level, and sex with tau deposition and tau-mediated metabolic dysfunction in older Adults. JAMA Netw Open 2019;2:e1913909.
45. Jansen WJ, Ossenkoppele R, Knol DL, et al. Prevalence of cerebral amyloid pathology in persons without dementia: a meta-analysis. JAMA 2015;313:1924–1938.
46. Lim YY, Mormino EC; Alzheimer's Disease Neuroimaging Initiative. APOE genotype and early β-amyloid accumulation in older adults without dementia. Neurology 2017; 89:1028–1034.
47. Wolf AB, Valla J, Bu G, et al. Apolipoprotein E as a β-amyloid-independent factor in Alzheimer's disease. Alzheimers Res Ther 2013;5:38.
48. Wang C, Najm R, Xu Q, et al. Gain of toxic apolipoprotein E4 effects in human iPSC-derived neurons is ameliorated by a small-molecule structure corrector. Nat Med 2018;24:647–657.
49. Shi Y, Yamada K, Liddelow SA, et al. ApoE4 markedly exacerbates tau-mediated neurodegeneration in a mouse model of tauopathy. Nature 2017;549:523–527.
50. Evans DA, Bennett DA, Wilson RS, et al. Incidence of Alzheimer disease in a biracial urban community: relation to apolipoprotein E allele status. Arch Neurol 2003;60:185–189.